Poiseuille advection of chemical reaction fronts: Eikonal approximation

Robert S. Spangler[a)] and Boyd F. Edwards
Department of Physics, West Virginia University, Morgantown, West Virginia 26506-6315

(Received 4 November 2002; accepted 24 December 2002)

An eikonal equation including fluid advection is derived from the cubic reaction-diffusion-advection equation, and is used to investigate the speeds and shapes of chemical reaction fronts subject to Poiseuille flow between parallel plates. Although the eikonal equation is usually regarded as valid when the front thickness is small compared to the radius of curvature of the front and to the size of the system, it is also found to be valid when the reaction front is thick with respect to the gap width. This new regime of applicability of the eikonal equation is consistent with its derivation, which requires only that the reaction front curvature and the fluid velocity vary negligibly across the front. The front distortion and the front speed increase with increasing η, defined as the ratio of the gap half-width to the reaction front thickness. Analytical limits of the front distortion and front velocity for small and large η are compared with general numerical results. © *2003 American Institute of Physics.* [DOI: 10.1063/1.1553752]

I. INTRODUCTION

In a solution of iodate and arsenous acid, with arsenous acid in stoichiometric excess, the iodide concentration $C = C(x,t) = [\mathrm{I}^-]$ evolves according to the reaction-diffusion-advection equation,[1,2]

$$\frac{\partial C}{\partial t} + \mathbf{V}\cdot\nabla C = D_C \nabla^2 C - \alpha C(C-C_2)(C-C_3), \tag{1}$$

where $C_2 = [\mathrm{IO}_3^-]_0$ denotes the initial iodate concentration, $C_3 = -k_a/k_b$ is a ratio of rate constants, and $\alpha = k_b[\mathrm{H}^+]^2$. The chemical reaction front serves to take C from its initial value $C=0$ far ahead of the front to the final value $C=C_2$ far behind the front. Surfaces of constant concentration describe the shape of the reaction front.

An advection-free eikonal equation

$$U_n = U_0 + D_C K \tag{2}$$

was derived by Tyson and Keener,[3] where U_n is the component of the front velocity normal to the surface of the front, U_0 is the speed of a flat front in the absence of advection, D_C is the molecular diffusivity, and K is the curvature of the front. In the present paper, we use Eq. (1) to derive an eikonal equation that includes advection, and use this equation to study the advection of chemical reaction fronts by Poiseuille flow between parallel plates. The predicted front speeds and distortions from the eikonal equation are compared with the predictions of the reaction-diffusion-advection equation.

II. GENERAL DERIVATION OF EIKONAL EQUATION

Surfaces of constant concentration define the reaction front, and move through the fluid as the reaction front propagates. The gradient of the concentration, ∇C, is perpendicular to such surfaces, so the unit vector pointing normally away from such a surface toward the unreacted fluid is given by

$$\hat{n} = -\frac{\nabla C}{|\nabla C|}. \tag{3}$$

Equation (3) represents the local direction of propagation of the chemical reaction front. The curvature of a surface of constant concentration, taken to be positive when the center of curvature is in the unreacted fluid, is

$$K = -\nabla\cdot\hat{n}. \tag{4}$$

A point $x(t)$ that remains on a surface of constant concentration as it travels with the front must satisfy $C(x(t),t) = \text{constant}$, whose total time derivative gives an evolution equation for the front,

$$\frac{dC}{dt} = \frac{\partial C}{\partial t} + \frac{d\mathbf{x}}{dt}\cdot\nabla C = 0. \tag{5}$$

Equations (3) and (5) allow us to express the normal component of velocity of a surface of constant concentration, $U_n = \hat{n}\cdot d\mathbf{x}/dt$, as

$$U_n = \frac{1}{|\nabla C|}\frac{\partial C}{\partial t}. \tag{6}$$

At each point in the fluid, Eqs. (3), (4), and (6), respectively, determine the unit normal vector, the curvature, and the normal velocity of the surface of constant concentration which passes through that point. Accordingly, Eq. (1) becomes

$$U_n = V_n + D_C\left(K - \frac{C''}{C'}\right) + \alpha\frac{C}{C'}(C-C_2)(C-C_3), \tag{7}$$

where $V_n = \hat{n}\cdot\mathbf{V}$ is the normal component of the fluid velocity, n is the normal coordinate measured as positive in the $+\hat{n}$ direction, a prime denotes the normal derivative $\hat{n}\cdot\nabla$

[a)]Electronic mail: bob_spangler_jr@yahoo.com

$=\partial/\partial n$, and $C'=\hat{n}\cdot\nabla C=-|\nabla C|$ is always negative because the concentration always decreases in the normal direction.

For a static fluid ($V_n=0$), Eq. (7) admits a steady one-dimensional solution[1]

$$C(n)=\frac{C_2}{1+e^{kn}} \tag{8}$$

with planar surfaces of constant concentration ($K=0$) that propagate in the fixed $+\hat{n}$ direction with velocity $U_n=U_0$, where $U_0=(\alpha D_C/2)^{1/2}(C_2-2C_3)$ is the velocity of a flat front in a static fluid. The associated decay constant is $k=(\alpha/2D_C)^{1/2}C_2$. Here $n=0$ identifies the surface of constant concentration $C=C_2/2$, midway between the initial and final concentrations $C=0$ (for $n\to+\infty$) and $C=C_2$ (for $n\to-\infty$), at the inflection point of the concentration profile, where $C''=0$. As such, $n=0$ identifies the surface of constant concentration at the center of the reaction front. Since $C_3/C_2\approx-2\times10^{-3}$, we can ignore C_3 to easily obtain the reaction front thickness $d=1/k=D_C/U_0$.[2]

When the fluid velocity V_n and front curvature K are nonzero but can be considered to be independent of n, Eq. (8) satisfies Eq. (7) with $k=(\alpha/2D_C)^{1/2}C_2$ as before, but the normal velocity now contains contributions from the curvature and the fluid velocity,

$$U_n=U_0+D_CK+V_n. \tag{9}$$

This is the desired eikonal equation augmented to include fluid advection. Equation (9) was inferred, but not derived, in Ref. 4, and allows for curved reaction fronts (with $\hat{n}$ varying from point to point on the fronts). It applies when the front thickness $d=D_C/U_0$ is small compared with both the radius of curvature $1/K$ and the scale of variations of the fluid velocity. As shown in the following, it also applies more generally, as long as V_n and K vary negligibly across the front, as assumed at the beginning of this paragraph.

III. APPLICATION TO POISEUILLE FLOW

Steady two-dimensional flow between parallel no-slip plates at $x=\pm a/2$ assumes the Poiseuille velocity[5,6]

$$\mathbf{V}(x,y,z,t)=6\left(\frac{1}{4}\frac{x^2}{a^2}\right)[V(y,z,t)\hat{y}+W(y,z,t)\hat{z}], \tag{10}$$

whose average over the gap (x direction) is

$$\overline{\mathbf{V}}(y,z,t)=V(y,z,t)\hat{y}+W(y,z,t)\hat{z}. \tag{11}$$

We specify $+\hat{z}$ as the direction of propagation of a front whose $y-z$ profile is a straight line parallel to the y-axis, and therefore consider K and V_n to be independent of y. We also consider the simplest possible fluid flow, with V and W being constant in time and uniform in space, so that $\mathbf{V}$ in Eq. (10) retains only the parabolic Poiseuille dependence on x. Accordingly denoting the position of the front by $z=H(x,t)$, we can determine the unit normal vector pointing into the unreacted fluid from

$$\hat{n}=\frac{\hat{z}-\hat{x}\dfrac{\partial H}{\partial x}}{\left[1+\left(\dfrac{\partial H}{\partial x}\right)^2\right]^{1/2}}. \tag{12}$$

We can then use Eq. (4), $V_n=\hat{n}\cdot\mathbf{V}$, and $U_n=\hat{n}\cdot\hat{z}(\partial H/\partial t)$ to write Eq. (9) as

$$\frac{\partial H}{\partial t}=U_0\sqrt{1+\left(\frac{\partial H}{\partial x}\right)^2}+\frac{3}{2}\left(1-\frac{4x^2}{a^2}\right)W+D_C\frac{1}{1+\left(\dfrac{\partial H}{\partial x}\right)^2}\frac{\partial^2 H}{\partial x^2}. \tag{13}$$

Defining dimensionless variables according to $x=(a/2)x'$, $t=(a/2U_0)t'$, and $H(x,t)=(a/2)h(x',t')$, and then dropping the primes allows us to write the dimensionless form of the eikonal equation as

$$\frac{\partial h}{\partial t}=\sqrt{1+\left(\frac{\partial h}{\partial x}\right)^2}+\frac{3}{2}(1-x^2)\epsilon+\frac{1}{\eta}\frac{1}{1-\left(\dfrac{\partial h}{\partial x}\right)^2}\frac{\partial^2 h}{\partial x^2}, \tag{14}$$

where $\epsilon=W/U_0$ is the ratio of the average fluid velocity to the front velocity and η is the ratio of the gap half-width to the front thickness. Equation (14), the focus of this paper, describes the front evolution in the eikonal limit with Poiseuille flow. The purpose of this paper is to compare the predictions of Eq. (11) with those of the dimensionless reaction-diffusion-advection equation for Poiseuille flow,

$$\frac{\partial c}{\partial t}+\frac{3}{2}\epsilon(1-x^2)\frac{\partial c}{\partial z}-\frac{1}{\eta}\left(\frac{\partial^2 c}{\partial x^2}+\frac{\partial^2 c}{\partial z^2}\right)+2\eta c^2(1-c), \tag{15}$$

where $c(x,t)$ is the concentration in units of C_2.

IV. NARROW GAP LIMIT $\eta\to0$

Many useful limits of Eq. (14) are accessible to analytic methods. These limits are considered here, and are compared with a numerical treatment described in Sec. VI. For these limits, we consider solutions that propagate without changing shape at constant velocity,

$$u=\frac{\partial h}{\partial t}. \tag{16}$$

We assume that we can expand u and h in powers of η according to

$$u=u_0+u_1+u_2+\cdots,\qquad h=h_0+h_1+h_2+\cdots, \tag{17}$$

where u_0 is independent of η, u_1 is proportional to η, and u_2 is proportional to η^2.

To lowest order (order η^{-1}),

$$\frac{1}{\eta}\left(1+\left(\frac{\partial h_0}{\partial x}\right)^2\right)^{-1}\frac{\partial^2 h_0}{\partial x^2}=0. \tag{18}$$

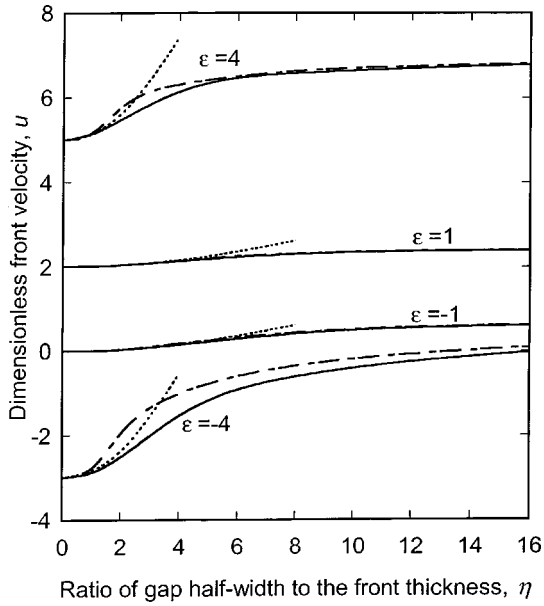

FIG. 1. A comparison of the front velocities predicted by the full reaction-diffusion-advection equation (solid traces), the eikonal approximation (chain-dashed traces), and the analytical limit of the eikonal equation valid for small η (dashed traces), where η is the ratio of the gap half-width to the front thickness, for $\epsilon=-4$, -1, 1, and 4, where ϵ is the ratio of the average flow velocity to the reaction front speed. The $\eta=0$ values for all three traces are determined by the small-η limit.

The natural implication is that

$$\frac{\partial^2 h_0}{\partial x^2}=0 \Rightarrow h_0=Ax+B, \tag{19}$$

where A and B are constants of integration. The boundary conditions

$$h_0'|_{x=\pm 1}=0 \tag{20}$$

imply that $A=0$. Thus the front assumes a flat zeroth-order profile with $h_0=\text{const}$.

In zeroth order, Eq. (14) becomes

$$u_0=1+\frac{3}{2}\epsilon(1-x^2)+\frac{1}{\eta}\frac{\partial^2 h_1}{\partial x^2}. \tag{21}$$

Integrating once yields

$$u_0 x=x+\frac{3}{2}\epsilon x-\frac{1}{2}\epsilon x^3+\frac{1}{\eta}\frac{\partial h_1}{\partial x}+D. \tag{22}$$

By evaluating Eq. (22) at $x=1$, then adding these equations, we find that $D=0$ and that the zeroth-order front velocity is

$$u_0=1+\epsilon. \tag{23}$$

This small-η result agrees with the corresponding limit of the reaction-diffusion-advection equation.[6] Since it is not possible to obtain results for $\eta=0$ numerically, Eq. (23) is used to complete the numerical curves at $\eta=0$ in Fig. 1.

In addition to knowing the limiting value of the front speed for $\eta\to 0$, the trend of the curve as η is slightly increased from zero is obtainable by linearizing the eikonal equation. Thus, the numerical results in the small-η regime can be checked analytically. First, we try to determine the linear η dependence of the front speed. The first-order component of Eq. (14) is

$$u_1=\frac{1}{\eta}\frac{\partial^2 h_2}{\partial x^2}. \tag{24}$$

Integrating once and applying the boundary conditions to solve for the constant of integration shows that the first-order correction to the front speed is zero. Thus,

$$u_1=0.$$

We now consider the second-order expansion of the eikonal equation,

$$u_2=\frac{1}{2}\left(\frac{\partial h_1}{\partial x}\right)^2-\frac{1}{\eta}\left(\frac{\partial h_1}{\partial x}\right)^2\frac{\partial^2 h_1}{\partial x^2}+\frac{1}{\eta}\frac{\partial^2 h_3}{\partial x^2}. \tag{26}$$

Inserting Eq. (23) into Eq. (22) gives

$$\left(\frac{\partial h_1}{\partial x}\right)^2=\left(\frac{\epsilon\eta}{2}\right)^2(x^6-2x^4+x^2). \tag{27}$$

Thus, Eq. (26) is

$$u_2=\left(\frac{\epsilon\eta}{2}\right)^2\left[\left(-\frac{3\epsilon}{2}\right)x^8+\left(\frac{1}{2}+\frac{7\epsilon}{2}\right)x^6-\left(1+\frac{5\epsilon}{2}\right)x^4+\left(\frac{1}{2}+\frac{\epsilon}{2}\right)x^2\right]+\frac{1}{\eta}\frac{\partial^2 h}{\partial x^2}. \tag{28}$$

Integrating once and satisfying the boundary condition at the edge of the front (as before) shows that the velocity of the front is

$$u=1+\epsilon+\left(\frac{1}{105}\right)(\epsilon\eta)^2. \tag{29}$$

Thus the front velocity near $\eta=0$ is quadratic in η. Equation (29) is also consistent with our observations that the small-η region of the curves in Fig. 1 all have positive curvature, and this curvature increases with increasing $|\epsilon|$. Equation (29) is represented by the dashed traces in Fig. 1.

Since the zeroth-order height is a constant, any distortion to the front profile must be described using at least the first-order correction to the height. By taking the square root and integrating Eq. (27), we can express the correction to the flat front profile as

$$h_1(x)=\frac{\epsilon\eta}{2}\left(\frac{x^4}{4}-\frac{x^2}{2}\right)+\text{const}. \tag{30}$$

the profiles for $\epsilon=1$, $\eta=1$, 4, 8, and 16 are shown in Fig. 2. Defining the distortion Γ as the ratio of the front height to the gap width, we see that, for small η,

$$\Gamma(\epsilon,\eta)=\frac{\epsilon\eta}{16}. \tag{31}$$

The distortions are plotted as a function of η in Fig. 3.

V. WIDE GAP LIMIT, $\eta\to\infty$

Also accessible to analytic methods is the asymptotic behavior as $\eta\to\infty$. It was found in Ref. 6 that, in this limit,

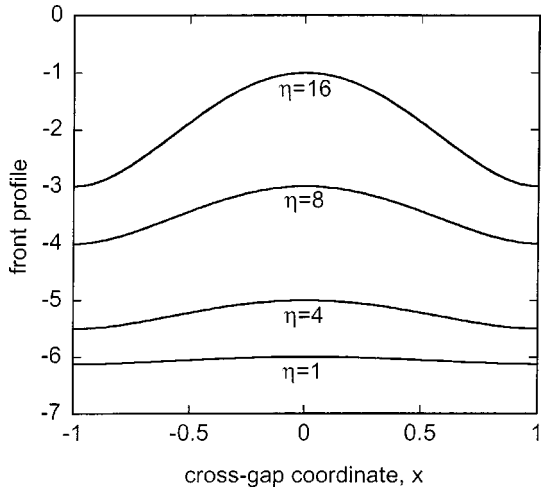

FIG. 2. Front profiles for $\epsilon=1$ and for $\eta=1$, 4, 8, and 16. The distortion and the curvature of the profile increases with increasing η.

there is a pronounced asymmetry between the shape and velocity of the front for supportive flow ($\epsilon>0$) in the direction of propagation and adverse flow ($\epsilon<0$) in the opposite direction. In the limit of large η, regions of sharp curvature occur at $x=\pm 1$ for $\epsilon>0$ and at $x=0$ for $\epsilon<0$, and the problem is rendered singular. Fortunately, the slope and curvature of the front both vanish at $x=0$ for $\epsilon>0$, and at $x=\pm 1$ for $\varepsilon<0$ in this limit. Evaluating Eq. (14) at these points accordingly gives the corresponding front speeds

$$\lim_{\eta\to\infty} u=1+\tfrac{3}{2}\epsilon \tag{32}$$

for $\epsilon>0$, and

$$\lim_{\eta\to\infty} u=1 \tag{33}$$

for $\epsilon<0$. A detailed discussion of the wide-gap results is presented in Ref. 7.

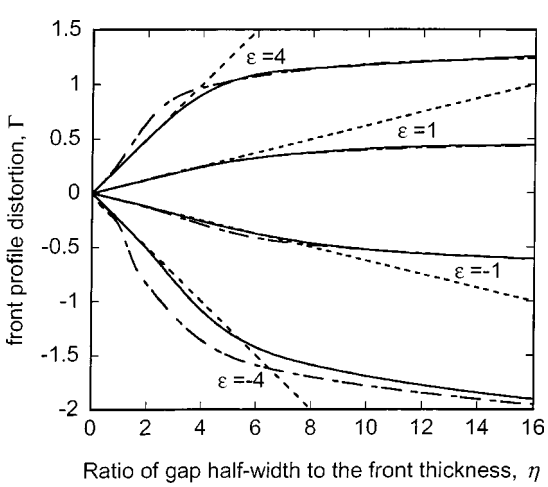

FIG. 3. Front profile distortion Γ, defined as the ratio of the front height to the width, vs η for $\epsilon=-4$, -1, 1, and 4. The results from the full advection-diffusion-reaction equation are shown with the solid trace, from the eikonal equation with the chain-dashed trace, and from the small-η analytical curve with the dashed trace.

VI. NUMERICAL TREATMENT OF THE EIKONAL EQUATION

Finite difference simulations were performed to explore the eikonal approximation. The number of grid points used was always greater than or equal to 16η. The front was allowed to evolve until u approached a constant value, and the time step used was such that decreasing the interval did not effect the steady-state value of u. A comparison between the front speeds predicted by Eq. (14) (dotted traces) and the full reaction-diffusion-advection equation[6] (solid traces predicted by Eq. (1)—see Ref. 6 for computational details) are shown in Fig. 1 for $\epsilon=-4$, -1, 1, and 4. Also shown are analytical results for small η [chain-dashed traces, Eq. (29)]. The reaction-diffusion-advection equation and the eikonal equation agree with each other for both large and small η, and with the small-η analytical results. The general agreement in the mid-range is surprising and interpreted as an added bonus. The two curves are nearly indistinguishable for $\epsilon=-1$ and $\epsilon=1$. The curves differ by 10% for the $\epsilon=4$ case, and the curves differ by at most 20% for the $\epsilon=-4$ case. Similar agreement is shown in the plots of distortion versus η for various values of ϵ (Fig. 3). The values of ϵ and η used for the distortion plots are the same as for the plots of the front speed. That the agreement is poorer for greater values of flow (expressed as the dimensionless variable ϵ) is not surprising, since greater flow leads to greater distortion, which leads to less favorable conditions for applying the eikonal equation (see Fig. 2). Also shown in the plots are the analytical limits for small η.

VII. SUMMARY

The striking agreement between the results produced by the full treatment and the eikonal treatment permits using the simpler model to predict experimental results, especially for small-amplitude flows. Not only is the eikonal treatment valid in the large-η regime, it is valid in the small-η regime and modestly valid in the mid-η regime. The difference between the eikonal equation results and advection-diffusion-reaction results increases with the magnitude of the gap averaged flow speed. This is expected, as a greater flow speed produces more distortion in the shape of the reaction front, and accordingly reduces the validity of the eikonal approximation.

The eikonal equation agrees with the reaction-diffusion-advection equation for both small and large η. Agreement for large η is expected because the reaction front is thin compared with all other length scales in this limit, and the eikonal equation is known to be valid under these conditions. In contrast, agreement for small η is surprising because the eikonal equation does not generally serve as a reliable approximation to the reaction-diffusion-advection equation when the reaction front thickness is comparable to or larger than other length scales of the problem. Close examination of the assumptions of our derivation and the boundary conditions allows us to understand why the eikonal equation applies for small η in this case. Our derivation of the eikonal equation (Sec. II) assumes only that the front curvature and the fluid velocity vary negligibly across the front, in the direction nor-

mal to the front. The boundary conditions demand that the front surface be normal to the bounding surfaces at $x=\pm 1$. When the reaction front is thick compared to the gap width (small η), lateral molecular diffusion of the catalyst species reduces the distortion of the front, so that front surfaces of constant concentration are all approximately planar (see Fig. 2). Since the steady Poiseuille fluid velocity does not vary with the propagation direction z, and since the front normal direction coincides approximately with the direction of propagation for small η owing to the reduced distortion, the limit of small η satisfies the required condition that the fluid velocity and the front curvature vary negligibly across the front. Since this condition also applies for steady front propagation in a cylinder, we expect the eikonal approximation to also apply in this geometry for small η. These calculations are under way.

ACKNOWLEDGMENTS

The authors thank J. W. Wilder for helpful discussions, and R.S.S. thanks Dr. Earl Scime for years of helpful instruction.

[1] A. Saul and K. Showalter, in *Oscillations and Traveling Waves in Chemical Systems*, edited by R. J. Field and M. Burger (Wiley, New York, 1985), p. 419; A. Hanna, A. Saul, and K. Showalter, J. Am. Chem. Soc. **104**, 3838 (1982).
[2] J. Huang and B. F. Edwards, Phys. Rev. E **54**, 2620 (1996).
[3] J. J. Tyson and J. P. Keener, Physica D **32**, 327 (1988).
[4] B. F. Edwards, J. W. Wilder, and K. Showalter, Phys. Rev. A **43**, 749 (1991).
[5] L. D. Landau and E. M. Lifshitz, *Course of Theoretical Physics: Fluid Mechanics* (Pergamon, New York, 1987), Chap. II.
[6] B. F. Edwards, Phys. Rev. Lett. **89**, 104501 (2002).
[7] B. F. Edwards, Chaos (to be published).